PERFORMANCE ANALYSIS OF DOWN SYNDROME DETECTION SYSTEM USING ULTRA SOUND FETUS IMAGES AND DEEP LEARNING CLASSIFICATION METHODS

V. Gokulakrishnan[1], Dr.S. Selvakumar[2*]

[1]*Research Scholar, Department of Computer and Science and Engineering, Dhanalakshmi Srinivasan University, Tiruchirappalli, Tamil Nadu, India.*
e-mail: gokulakrishnanv.phd2022@dsuniversity.ac.in,
orcid: https://orcid.org/0009-0003-9115-7969
[2*]*Professor, Department of Computer Science Engineering, Dhanalakshmi Srinivasan University, Samayapuram, Tiruchirappalli, Tamil Nadu, India.*
e-mail: 2ssksri@gmail.com, orcid: https://orcid.org/0009-0005-9820-3387

SUMMARY

Down Syndrome (DS) is a genetic disorder due to a partial copy of the 21 st chromosome in the fetus, usually detected by invasive techniques like Amniocentesis and Chorionic Villus Sampling (CVS) which have chances of miscarriage. This paper suggests a completely automated and computer-aided method of non-invasive detection of DS by ultrasound fetus (USF) images, as a way of overcoming the constraints of the conventional diagnostic methods. The proposed system applies Non-Sub Sampled Contourlet Transform (NSCT) in transforming the image, and extracting features and classifying them using a custom Convolutional Neural Network (CNET). The system was trained and tested with normal and abnormal USF images with considerable results. On the Mendeley data, the system had Fetal NT Sensitivity (FNSE) of 99.24, Fetal NT Specificity (FNSP) of 99.19, Fetal NT Accuracy (FNA) of 99.23, Fetal Positive predictive rate (FPPR) of 99.28, and Fetal Negative predictive rate (FNPR) of 99.24. In the case of Kaggle Fetus (KF) dataset, the system achieved FNSE of 99.24, FNSP of 99.33, FNA of 99.1, FPPR of 99.29, and FNPR of 99.26. Mendeley and KF datasets had the average Fetus Detection Time (FDT) of 0.51 ms and 0.46 ms, respectively. The results of this study prove that the proposed method performs better in terms of detection accuracy, sensitivity, and speed and is a promising tool to conduct early non-invasive screening of the fetus and minimize the use of invasive diagnostic methods.

Key words: *down syndrome, ultrasound imaging, deep learning, convolutional neural network, NSCT, fetus detection, prenatal screening.*

INTRODUCTION

Down Syndrome (DS) is a genetic disorder which can be occurred in the fetus due to the partial copy of chromosome 21 during the pregnancy time period. At the time of pregnancy of female, the DS has been identified through various identification testing procedure and diagnostic testing procedure [1][2][3]. The identification testing procedure initially identifies and determines the score of the chance of the DS occurrence on the fetus. The rank will be provided based on the score in this testing procedure. The

higher rank indicates the risk chance of DS is getting high and the lower rank indicates the risk chance of DS is getting low. The main limitation of this testing procedure is that it does not provide diagnosis result. The identification testing procedure can be done in health care centers by the expert physcian through three screening methodologies as First Trimester Screening (FTS), Second Trimester Screening (STS) and Non-Invasive Prenatal Screening (NIPS) [4][5][6]. In FTS, the blood from the mother has been analyzed to detect any marker signs and also check the fluid level of the neck of the fetus [7]. In STS, the blood from the mother only has been analyzed to detect the marker signs. In NIPS, the incidence of marker cells in the mother's blood has been analyzed to detect the DS. The screening accuracy level of this test is low and hence the alternative diagnostic method has been used at present. In this diagnostic testing procedure, the cells in the fetus have been analyzed, and its chromosomes have also been analyzed. This diagnostic testing procedure has been done through two tests as Amniocentesis and Chorionic Villus Sampling (CVS). In Amniocentesis diagnostic testing procedure, the fluid around the region of the fetus has been tested. In CVS diagnostic procedure, placenta has been tested [8][9][10]. When comparing with the identification testing procedure, the diagnostic testing procedure provides higher DS detection and identification rate and hence this method has been used at present through the expert radiologist [14]. This method has also certain limitation as it leads to miscarriage sometimes [11][12][13]. In order to avoid the limitations of these DS detection methods, the computer-aided screening methodologies using Ultra Sound Fetus (USF) images have been proposed in this article. Figure 1 (a) shows the normal USF image and Figure 1 (b) shows the abnormal USF image.
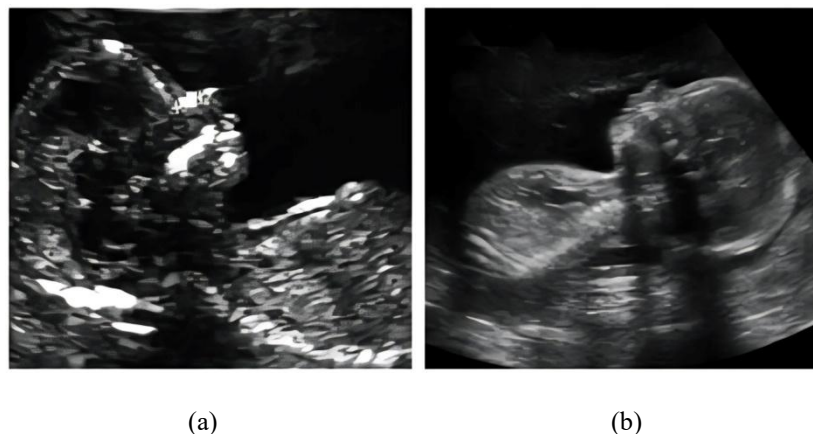

(a)   (b)

Figure 1. (a) Normal USF image (b) Abnormal USF image

Key Contribution

- Design of a totally computerized system of DS detection with USF images and the absence of invasive procedures.

- NSCT transformation is employed to transform the spatial USF images into a frequency domain image with a better ability of extracting features.

- The extraction of features and categorizing of fetus images as normal or abnormal by a Convolutional Neural Network (CNET) that is specifically trained to classify fetal images according to the extracted features.

- High detection accuracy and speed in two independent datasets (Mendeley and Kaggle Fetus), high FNSE, FNSP, FNA, and FPPR and FNPR of more than 99%.

- Computation of Fetus Detection Time (FDT) to estimate system efficiency with the results of 0.51 ms and 0.46 ms on Mendeley and KF dataset, respectively.

This article has been structured as section 2 states various DS detection methodologies using USF images, section 3 states the proposed DS framework modelling algorithm, section 4 details about the simulation results and finally the conclusion is given in section 5.

LITERATURE SURVEY

In recent developments of detection of Down Syndrome (DS) through ultrasound fetus (USF) images, several models of deep learning and image processing have been used. Nevertheless, the current methods still have significant weaknesses that the research is expected to fill. The study created a deep learning model of identification and classification of DS based on pregnancy ultrasound images [15][16][17]. Their system was able to reach high performance with FNSE of 98.27% and FNSP of 98.56% on the Mendeley dataset, and FNSE of 97.26% and FNSP of 97.36% on the KF dataset using fine-tuned texture features [18][19]. Although these results were promising, the method had a drawback that it relied on texture-based features, which might not be adequate to describe the complexity of fetal appearance especially in difficult cases when the images have low-resolution or are rough [20][21]. Moreover, although the research has indicated competitive performance, the model generalization to a wide range of datasets of different image quality is not addressed, in general, yet [22][23]. Another method of non-invasive DS detection that was used by the previous study is the analysis of features and the computer-aided classification. They obtained FNSE of 97.98% and FNSP of 97.87% on the Mendeley dataset but the model performed poorly on the KF dataset (FNSE: 96.87%) [24][25]. This inconsistency indicates that dataset variability is sensitive to the model's strength, suggesting differences in the flexibility of detection systems across different types of ultrasound images.

The Swin Transformer (ST) architecture, which was presented as a method for DS detection and unites segmentation and alignment tasks in a single framework, was introduced. On the Mendeley dataset, they obtained FNSE of 97.17% and KF data of 96.14%. Nevertheless, the approach that depends on the segmentation mechanism within one network may also enhance the complexity and computing cost, and the model is not as efficient in real-time application. Furthermore, unlike other models, the model does not have total consideration on the sensitivity of the image quality and noise and this may inhibit its performance in clinical practice. The previous study investigated modified machine learning methods applied on low-resolution USF images to ensure that it remains resistant to image degradation. Although the FNSE of 96.87% was obtained on Mendeley images, the accuracy showed a considerable decrease in KF images on the FNSE (94.98%). This implies that current approaches fail to be very accurate in comparing image resolutions and other variables, which implies that more powerful feature extraction and classification strategies are required.

Although these studies show that deep learning and machine learning models are promising in detecting DS, they still have a number of limitations, including sensitivity to image quality, lower performance in low-resolution images, and computing viability. To solve these problems, the given work proposes the combination of Non-Sub Sampled Contourlet Transform (NSCT) as the tool of high-quality feature extraction and a dedicated Convolutional Neural Network (CNET) framework that guarantees enhanced performance, efficiency, and stability in a wide range of fetal ultrasound images.

PROPOSED METHODOLOGIES

This research work proposes a fully automated and computer assisted methodologies for the detection of DS using fetus analysis method. This proposed work contains Non sub Sampled Contourlet (NSCT) transformation, fetus feature computation process and the proposed CNET classification architecture. It has been functioned with respect to both training and testing phases. In case of training the system, both normal and abnormal USF images have been trained through the functional modules of NSCT and fetus feature extraction to generate the training vector. In case of testing the system, the test USF image has been classified through the functional modules of NSCT and fetus feature extraction along with the trained vectors.

Figure 2 (a) shows the USF image training process and Figure 2 (b) shows the USF image testing process.
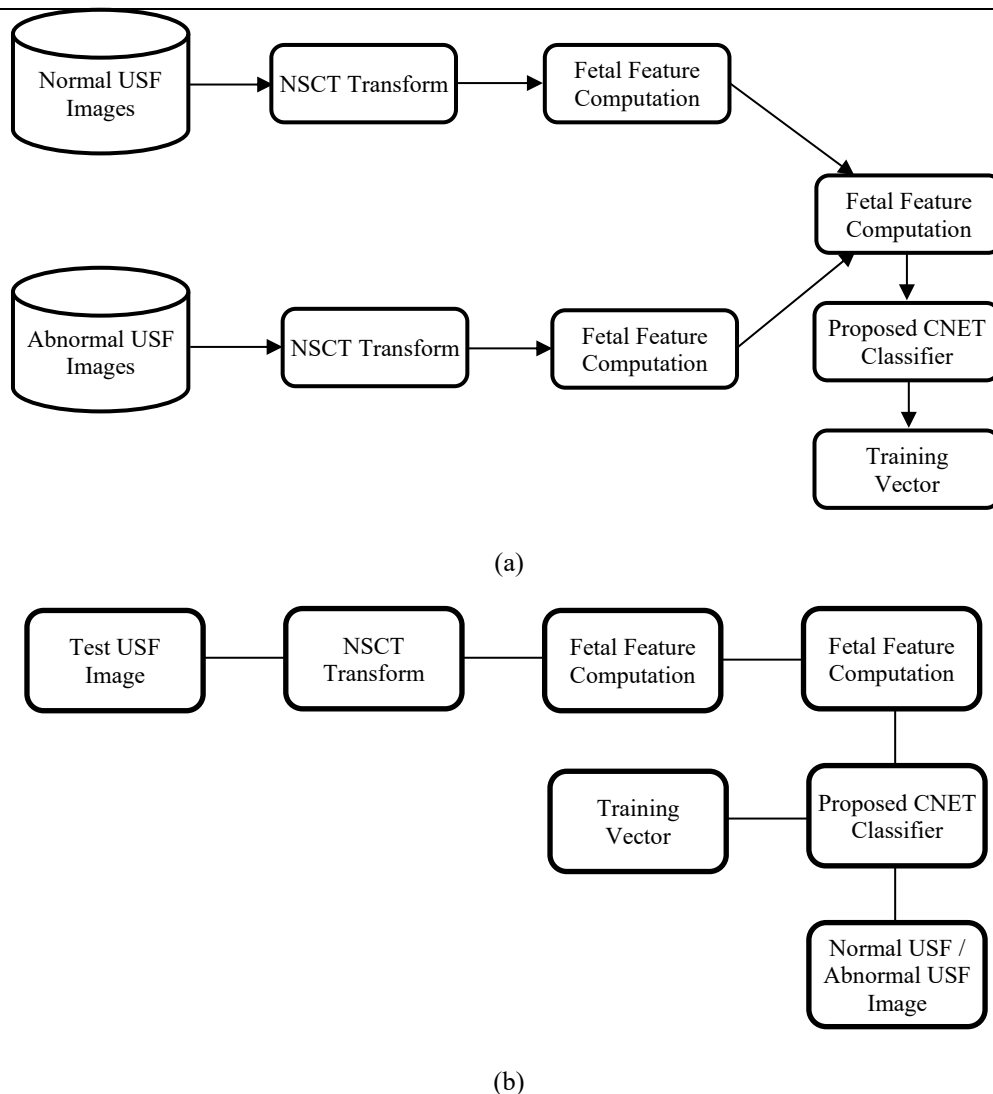
(a)

(b)

Figure 2. (a) USF image training process (b) USF image testing process

NSCT Transformation Process

Most of the deep learning algorithms used spatial fetus images for both training and classification process and hence its fetus image classification result is not getting optimum. In order to improve the fetus image classification results, the deep learning algorithm should be fed with the frequency fetus image. Therefore, it is important for transforming the input source spatial USF image into the frequency USF image through the transformation process. Even though lot of transformation process are available to perform this transformation such as Discrete Wavelet Transform (DWT), Gabor Wavelet Transform (GWT) and Curvelet Transform (CT), its decomposition error rate during the transformation process is high which affects the huge impact on the final USF image classification results. Hence, the transformation with low error rate has been required for obtaining the frequency USF image from the spatial USF image. This research work uses Non-Sub Sampled Contourlet Transform (NSCT) for performing this spatial USF into frequency USF image. The internal structure of the NSCT has been depicted in Figure 3.

The NSCT produces one Low Pass Fetus (LPF) sub band and two High Pass Fetus (HPF) sub bands and all these three sub bands are integrated into a two-dimensional matrix and it has been further used in this work to extract the fetus features for obtaining the fetus classification results.
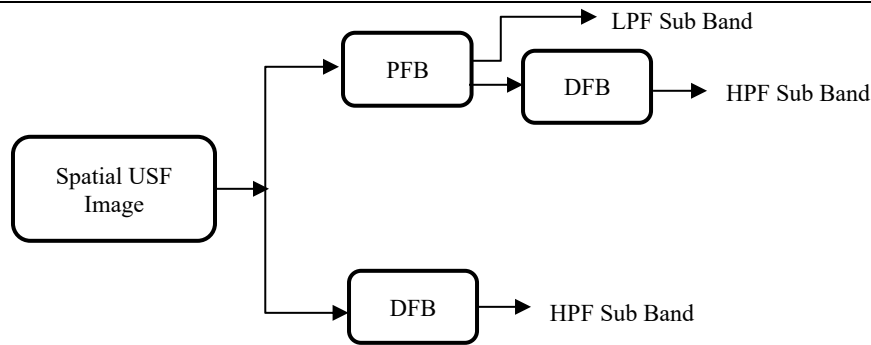
Figure 3. USF image decomposition through NSCT

Fetus Feature Computation Process

Features are the texture patterns which are computed from the image at either any angle of orientation or any direction of pixels. These computed texture features from the image are helpful for analyzing various components within the image. The computed features are in frequency domain pattern and they are directly fed into any type of classifier for producing the required classification results. The features are the pivotal for fetus image classification process. It computes the information from the USF images and further they can be used by the classifier to differentiate the normal USF image from the abnormal USF image. This research work computes the pivotal features from the set of normal USF images and the set of abnormal USF images during the training level of the proposed classifier. At this level of classifier training process, the trained features are generated. After training the classifier, the pivotal features from the test fetus image have been computed and these fetus pivotal features are classified with respect to the trained fetus images. The following mathematical equations describe the pivotal fetus features from the USF image.

Fetus Energy Rate (FER): Equation 1 adds the squared pixel values in the transformed image to calculate the total energy of the fetus image.

$$Fetus\ Energy\ Rate\ (FER) = \sum_{i=1}^{M-1}\sum_{j=1}^{N-1} S^2(i,j) \tag{1}$$

Where as $S(i,j)$ is the fetus sub band image through NSCT transformation process, i and j corresponds to the row and column of the fetus sub band image.

Fetus Contrast Rate (FCR): Refines the disparity between the pixel values in the transformed image considering the spatial distribution of the pixel values are shown in equation 2.

$$Fetus\ Contrast\ Rate\ (FCR) = \sum_{i=1}^{M-1}\sum_{j=1}^{N-1} S(i,j) * (i-j)^2 \tag{2}$$

Fetus Dissimilarity Rate (FDR): Equation 3 calculates the dissimilarity between pixel values by taking into account, their absolute differences of spatial locales.

$$Fetus\ Dissimilarity\ Rate\ (FDR) = \sum_{i=1}^{M-1}\sum_{j=1}^{N-1} S(i,j) * |i-j| \tag{3}$$

Fetus Heuristic Rate (FHR): The normalized total of pixel values of the total image intensity are shown in equation 4.

$$Fetus\ Heuristic\ Rate\ (FHR) = \frac{\sum_{i=1}^{M-1}\sum_{j=1}^{N-1} S(i,j)}{i*j} \tag{4}$$

Fetus Higher Order rate (FHOR): The higher order interaction of the pixel values divided by the squares of the spatial distances are shown in equation 5.

$$Fetus\ Higher\ Order\ Rate\ (FHOR) = \frac{\sum_{i=1}^{M-1}\sum_{j=1}^{N-1} S(i,j)}{(i+1)^2(j+1)^2} \tag{5}$$

Fetus Lower Order Rate (FLOR): Equation 6 computes low-order interactions of pixel values which are normalised by the squared spatial distance.

$$Fetus\ Lower\ Order\ Rate\ (FLOR) = \frac{\sum_{i=1}^{M-1}\sum_{j=1}^{N-1} S(i,j)}{(i-1)^2(j-1)^2} \tag{6}$$

All these computed fetus pivotal features from the test USF image are stored in a 2D-matrix and they are indexed as Fetus Feature Vector (FFV) by indexing row and column. This computed FFV has been given to the proposed deep learning algorithm for generating the required classification results in this research work.

Classifications

The proposed Convolutional Fetus Network (CNET) architecture for the classifications of the USF images is given in Figure 4. This architecture contains three numbers of CNET modules named as CNET1, CNET2 and CNET3 and they are followed by Fully Connected Neural Network (FCNN) module which is necessary to produce the fetus image classification results. The main objective of each CNET module in this architecture is to produce a greater number of internal fetus features which can be combined with the previous module input and output. This increases the size of the generated features which is the main reason for obtaining the higher fetus image classification results.
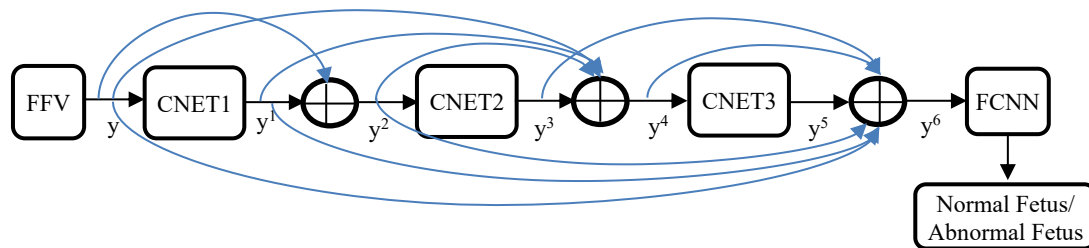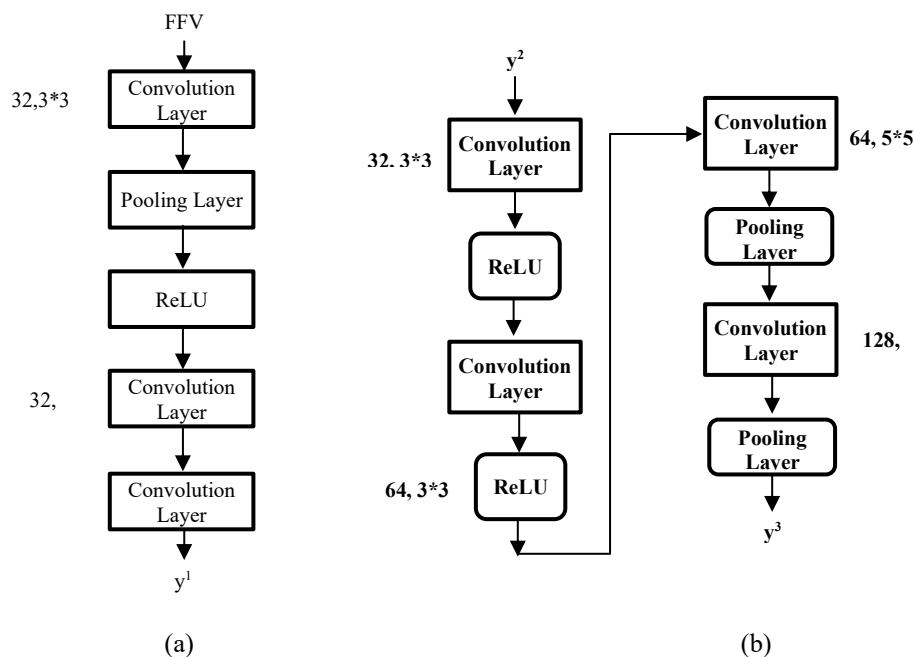

Figure 4. Proposed CNET architecture for the classifications of the USF images
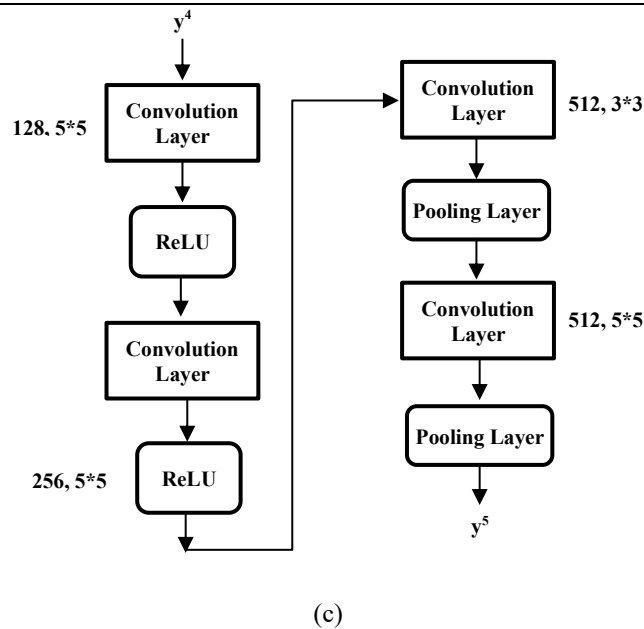

(a)

(b)

(c)

Figure 5. (a) Structure of CNET1 (b) Structure of CNET2 (c) Structure of CNET3

The CNET1 structure consists of two independent Convolution layers and two functional pooling layers and ReLU layer. The FFV data has been passed through the Convolution layer which has been designed with 32 filters and sized as 3*3 and its output pattern has been resized using pooling layer. The negative responses in the pooling layer output have been eliminated by ReLu and its output has been passed through the second Convolution layer which has been designed with 32 filters and sized as 5*5 and its output is designated as y1, as illustrated in Figure 5(a).

The entire functional operation of CNET1 module has been depicted in the following Equation 7.

$$y1 = CNET1(FFV, C1, C2) \tag{7}$$

Where, C1 and C2 are the first and second Convolution layers and they are also given in the following Equations 8 and 9.

$$C1: \{32 \ filters \ and \ 3*3 \ size\} \tag{8}$$

$$C2: \{32 \ filters \ and \ 5*5 \ size\} \tag{9}$$

The output data of the first CNET1 has been added with its input data and it is given in the following Equation 10.

$$y2 = y1 + y \tag{10}$$

Whereas, y1 is the output responses of CNET1 and y1 is the input data to the CNET1.

The CNET2 structure consists of four independent Convolution layers and two functional pooling layers and ReLU layer. The y2 data has been passed through the first Convolution layer which has been designed with 32 filters and sized as 3*3 and the negative responses in the pooling layer output have been eliminated by ReLu and its output has been passed through the second Convolution layer which has been designed with 64 filters and sized as 3*3 and the negative responses in this layer output have been eliminated by ReLu. Then it has been transformed through the third Convolution layer which has been designed with 64 filters and sized as 5*5 and its output pattern has been resized using pooling layer. This output is again transformed through the fourth Convolution layer which has been designed with 128 filters and sized as 3*3 and its output pattern has been resized using pooling layer and its output is designated as y3, as illustrated in Figure 5(b).

The entire functional operation of CNET2 module has been depicted in the following Equation 11.

$$y3 = CNET1(y2, C1, C2, C3, C4) \tag{11}$$

Where, C1, C2, C3 and C4 are the first, second, third and fourth Convolution layers and they are also given in the following Equations 12, 13, 14, 15.

$$C1: \{32 \; filters \; and \; 3*3 \; size\} \tag{12}$$

$$C2: \{64 \; filters \; and \; 3*3 \; size\} \tag{13}$$

$$C3: \{64 \; filters \; and \; 5*5 \; size\} \tag{14}$$

$$C4: \{128 \; filters \; and \; 3*3 \; size\} \tag{15}$$

The output data of the first CNET2 has been added with its previous modules input and data and it is given in the following Equation 16.

$$y4 = y3 + y2 + y1 + y \tag{16}$$

The CNET3 structure consists of four independent Convolution layers and two functional pooling layers and ReLU layer. The y4 data has been passed through the first Convolution layer which has been designed with 128 filters and sized as 5*5 and the negative responses in the pooling layer output have been eliminated by ReLu and its output has been passed through the second Convolution layer which has been designed with 256 filters and sized as 5*5 and the negative responses in this layer output have been eliminated by ReLu. Then it has been transformed through the third Convolution layer which has been designed with 512 filters and sized as 3*3 and its output pattern has been resized using pooling layer. This output is again transformed through the fourth Convolution layer which has been designed with 512 filters and sized as 5*5 and its output pattern has been resized using pooling layer and its output is designated as y5, as illustrated in Figure 5(c).

The entire functional operation of CNET3 module has been depicted in the following Equation 17.

$$y5 = CNET1(y4, C1, C2, C3, C4) \tag{17}$$

Where, C1, C2, C3 and C4 are the first, second, third and fourth Convolution layers and they are also given in the following Equations 18, 19, 20, 21.

$$C1: \{128 \; filters \; and \; 5*5 \; size\} \tag{18}$$

$$C2: \{256 \; filters \; and \; 5*5 \; size\} \tag{19}$$

$$C3: \{512 \; filters \; and \; 3*3 \; size\} \tag{20}$$

$$C4: \{512 \; filters \; and \; 5*5 \; size\} \tag{21}$$

The output data of the first CNET3 has been added with its previous modules input and data and it is given in the following Equation 22.

$$y6 = y5 + y4 + y3 + y2 + y1 + y \tag{22}$$

This proposed CNET architecture also contains FCNN layers in order to produce the fetus image classification results. The FCNN is designed with three internal FCNN sub layers and the first two FCNN sub layers contain 4096 biased neurons and the third FCNN sub layer contains 512 biased neurons. The feature value vector y6 has been passed through all these three sub layers of FCNN and the feature values in the final FCNN sub layer have been summed up to produce the final fetus image classification results. Figure 6(a) is final CNET classifier-based classification results of the normal USF images which don't

have any morphological symptoms for down syndrome and Figure 6(b) final CNET classifier-based classification results of the USF images which have the morphological symptoms for down syndrome. In addition to the ultrasound fetus image classification process, morphological algorithm has been used to segment the nasal bone in this work.

(a)

(b)
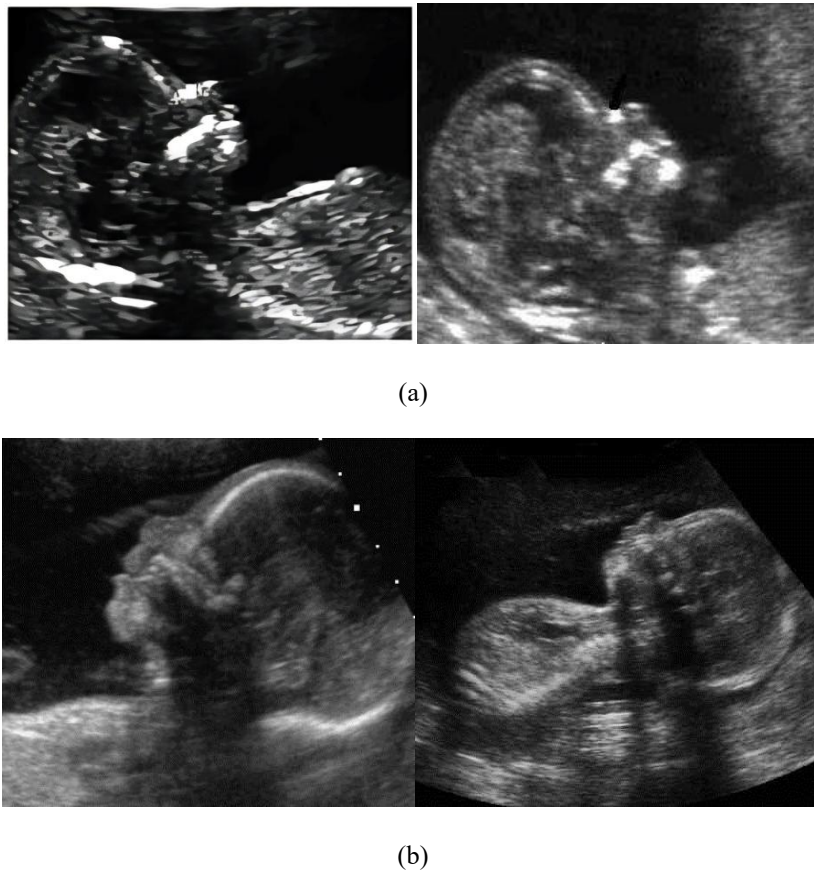
Figure 6. (a) Normal USF images (b) abnormal USF images

Algorithm 1: DS Detection Using Ultrasound Fetus Images

Input: training_images, training_labels: Labeled training USF images,   - test_images: Test USF images

Output: trained_model: Convolutional Neural Network (CNET) model,   - predictions: Predicted labels for test images

Step 1: Preprocessing

  Procedure apply_NSCT (image)

    transformed_image = NSCT (image) # Spatial to frequency domain

    Return transformed_image

Step 2: Feature Extraction

  Procedure extract_features(transformed_image)

    FER = $\sum [S(i,j)]^2$

    FCR = $\sum S(i,j) * (i-j)^2$

FDR = ∑ S(i,j) * |i-j|

FHR = ∑ S(i,j) / (i*j)

FHOR = ∑ S(i,j) / (i+1)^2 * (j+1)^2

FLOR = ∑ S(i,j) / (i-1)^2 * (j-1)^2

Return [FER, FCR, FDR, FHR, FHOR, FLOR]

Step 3: Classification

Procedure CNET_classifier(feature_vector)

Apply Conv2D, Flatten, Dense layers

Return output (normal/abnormal)

Step 4: Model Training

Procedure train_CNET (training_images, training_labels)

For each image, label:

Apply NSCT, extract features

Predict label, compute loss, update weights

Return trained_model

Step 5: Testing

Procedure test_CNET (test_images)

For each image:

Apply NSCT, extract features

Predict label

Return predictions

Main:

trained_model = train_CNET (training_images, training_labels)

predictions = test_CNET (test_images)

Print predictions

Down Syndrome (DS) is an algorithm (Algorithm 1) that transforms the images of the fetus in the ultrasound using Non-Sub Sampled Contourlet Transform (NSCT). Significant texture characteristics are obtained, including Fetus Energy rate (FER) and Fetus Contrast rate (FCR). The classification of these features is done on a Convolutional Neural Network (CNET). The model is trained on labeled images, and tested on unseen data in order to provide normal or abnormal classifications. The result is in the form of the trained model and predictions.

RESULTS AND DISCUSSIONS

This study software has been created with Python 3.7+ and deep learning with TensorFlow 2.x or PyTorch 1.x. Keras, OpenCV, NumPy, Matplotlib and Scikit-learn libraries are employed in the construction of models, image processing and evaluation. The system is optimized to use GPU and CUDA 11.x and cuDNN 8.x, which requires an NVIDIA CUDA-enabled card. They are based on two datasets: the Mendeley dataset containing 1,010 ultrasound fetus (USF) images (255 normal, 755 abnormal) and KF dataset containing 1,505 images (755 normal, 750 abnormal). Both data sets include pictures taken in the 1114 week of pregnancy, both sets with 512x512 and 256x256 pixels (Mendeley, KF). These are hand-labeled images in the case of detection of Down Syndrome. The Convolutional Neural Network (CNET) is trained at a learning rate of 0.001 on the Adam optimizer with a batch size of 32 and 50 epochs. To avoid overfitting, dropout will be 0.5. The structure of the model consists of convolutional layers with a different filter size (3x3 and 5x5) and fully connected layers that consist of 4096 and 512 biased neurons. Image normalization is used and the performance is measured in terms of the Fetal NT Sensitivity (FNSE), Specificity (FNSP), Accuracy (FNA), and Predictive Rates (FPPR, FNPR).

In this article, the DDS has been technically evaluated on two independent Fetus Imaging datasets Mendeley [20] and Kaggle Fetus (KF) [21] in order to measure the performance efficiency. Both the datset contains fetus images with NT region manually marked images. The Mendeley dataset has been constructed with Ultra Sound Fetus (USF) images which can be obtained in the period of 11-14 weeks trimester pregnancy time. The 1519 number of pregnancy female were involved in cosntructing this dataset at Shenzhen people's hospital-China. All these USF images are copywriting property and they permitted the USF images for any non-commercial research works. This Shenzhen people's hospital was collaborated with the Longhua Hospital-China in order to accquire number of USF images. From this open-access USF dataset, 255 normal USF images and 755 abnormal USF images have been taken for evaluating the performance efficiency of the proposed DDS in this article. All the USF images in this dataset are having the imaging resolution of 512*512 and they have been quantized with 16-bit resolution pattern.

The KF dataset has been constructed with USF images which can be obtained in the period of 11-14 weeks trimester pregnancy time. The 2500 number of pregnancy female were involved in cosntructing this dataset. All these USF images are copywriting property and they permitted the USF images for any non-commercial research works. From this open access USF dataset, 755 normal USF images and 750 abnormal USF images have been taken for evaluating the performance efficiency of the proposed DDS in this article. All the USF images in this dataset are having the imaging resolution of 256*256 and they have been quantized with 8-bit resolution pattern.

The nuchal translucency (NT) region in abnormal USF has been measured using the proposed DDS framework model and its performance has been computed using the following mathematical Equations.

Fetus NT Sensitivity (FNSE): It is the percentage of true positives (identifying an abnormal image correctly) out of all the true positives (true positives and false negatives) (equation 23).

$$Fetus\ NT\ Sensitivity\ (FNSE) = \frac{TP}{TP+FN} \tag{23}$$

Fetus NT Specificity (FNSP): Equation 24 is the number of true negatives who were really known to be normal images, per the number of true negatives (true negatives and false positives).

$$Fetus\ NT\ Specificity\ (FNSP) = \frac{TN}{TN+FP} \tag{24}$$

Fetus NT Accuracy (FNA): Equation 25 is the general accuracy of the model as it involves dividing the number of correctly classified images (true positives and true negatives) by the total number of images.

$$Fetus\ NT\ Accuracy\ (FNA) = \frac{TP+TN}{TP+TN+FP+FN} \tag{25}$$

Fetus Positive Predictive Rate (FPPR): Equation 26 is a measure of the true positives (correctly detected abnormal images) compared to all the predicted positives (true positives and false positives).

$$Fetus\ Positive\ Predictive\ Rate\ (FPPR) = \frac{TP}{TP+FP} \tag{26}$$

Fetus Negative Predictive rate (FNPR): Equation 27 is a ratio of the true negatives (correctly identified normal images) and all the negatives predicted (true negatives and false negatives).

$$Fetus\ Negative\ Predictive\ Rate\ (FNPR) = \frac{TN}{TN+FN} \tag{27}$$

Whereas, TP and TN correlate the number of pixels belonging to the segmented NT region of the abnormal USF images and the number of pixels belonging to the non-NT region of the abnormal USF images with respect to the correct. FP and FN correlate the number of pixels belonging to segmented NT region of the abnormal USF images and the number of pixels belonging to the non-NT region of the abnormal USF images with respect to incorrect.

Table 1 is the simulation assessment of the proposed DDS on Mendeley- USF images. The proposed DS detection methodologies have attained 99.24% FNSE, 99.19% FNSP, 99.23% FNA, 99.28% FPPR and 99.24% FNPR on the set of USF images in Mendeley dataset.

Table 1. Simulation assessment of the proposed DDS on mendeley- USF images

USF images	Results measured in %				
	FNSE	FNSP	FNA	FPPR	FNPR
1	98.9	99.4	98.8	98.7	98.4
2	99.2	99.6	99.4	99.1	98.9
3	99.5	98.3	99.3	99.7	99.4
4	99.1	98.7	99.7	99.4	99.1
5	99.2	98.9	99.4	99.3	99.6
6	99.6	99.4	99.2	99.1	99.5
7	99.3	99.8	99.4	98.9	99.3
8	99.1	99.4	99.1	99.5	99.7
9	99.2	99.1	98.9	99.4	99.1
10	99.3	99.3	99.1	99.7	99.4
Average	**99.24**	**99.19**	**99.23**	**99.28**	**99.24**

Table 2 is the simulation assessment of the proposed DDS on KF- USF images. The proposed DS detection methodologies have attained 99.24% FNSE, 99.33% FNSP, 99.1% FNA, 99.29% FPPR and 99.26% FNPR on the set of USF images in KF dataset.

Table 2. Simulation assessment of the proposed DDS on KF- USF images

USF images	Results measured in %				
	FNSE	FNSP	FNA	FPPR	FNPR
1	99.4	99.7	97.3	99.3	99.2
2	98.9	98.8	98.8	98.5	98.7
3	98.3	99.4	99.4	99.4	99.4
4	99.4	99.2	99.1	99.2	99.1
5	99.8	99.1	99.8	99.6	99.6
6	99.3	99.6	99.3	99.5	99.3
7	99.1	99.3	99.1	99.3	99.7
8	99.3	99.1	99.2	99.1	99.3
9	99.2	99.8	99.6	99.7	99.1
10	99.7	99.3	99.4	99.3	99.2
Average	**99.24**	**99.33**	**99.1**	**99.29**	**99.26**

Table 3 is the comparative evaluation of the proposed DDS framework by two USF datasets.

Table 3. Comparative evaluation of the proposed DDS framework by two USF datasets

Parameters	Mendeley- USF dataset	KF- USF dataset
FNSE	99.24	99.24
FNSP	99.19	99.33
FNA	99.23	99.1
FPPR	99.28	99.29
FNPR	99.24	99.26

Figure 7 (a) and Figure 7(b) show the graphical analysis of FNA with respect to epochs on Mendeley-USF dataset and KF- USF dataset respectively.
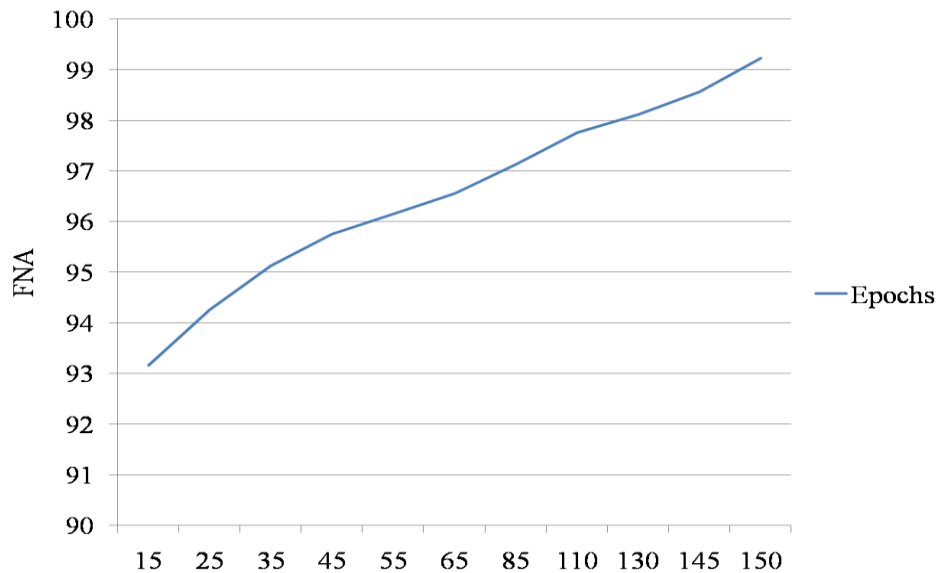
(a)
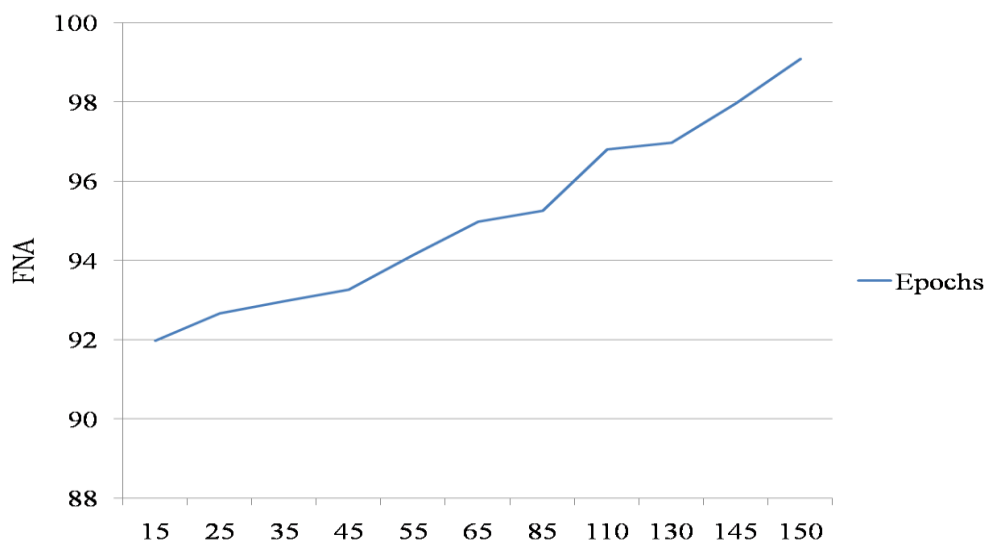
(b)

Figure 7. Graphical analysis of FNA with respect to epochs (a) Mendeley- USF dataset (b) KF- USF dataset

Table 4 is the comparative analysis of the proposed DDS framework with other similar traditional methodologies (Mendeley- USF dataset).

Table 4. Comparative analysis of proposed DDS framework with other similar traditional methodologies
(Mendeley- USF dataset)

Methodologies	FNSE	FNSP	FNA	FPPR	FNPR
Proposed DDS framework	**99.24**	**99.19**	**99.23**	**99.28**	**99.24**
Deep Learning-based Architecture	98.27	98.56	98.10	98.38	98.37
Non-invasive DS Detection	97.98	97.87	97.87	97.76	98.10
Swin Transformer for DS Detection	97.17	96.15	96.39	96.37	97.37
Modified Machine Learning Method	96.87	95.29	95.87	95.28	96.87
Deep Learning Measurement Model	95.27	95.10	94.38	94.86	95.56

Table 5 is the comparative analysis of the proposed DDS framework with other similar traditional methodologies (KF- USF dataset).

Table 5. Comparative analysis of proposed DDS framework with other similar traditional methodologies (KF- USF dataset)

Methodologies	FNSE	FNSP	FNA	FPPR	FNPR
Proposed DDS framework	**99.24**	**99.33**	**99.1**	**99.29**	**99.26**
Deep Learning-based Architecture	97.26	97.36	97.67	98.16	98.38
Non-invasive DS Detection	96.87	96.87	96.65	97.39	97.67
Swin Transformer for DS Detection	96.14	96.10	95.29	96.76	97.10
Modified Machine Learning Method	95.28	95.28	94.98	95.29	96.87
Deep Learning Measurement Model	94.98	94.29	94.16	94.45	95.27

Table 6 is the Fetus Detection Time (FDT) computations using the proposed DDS framework model- Mendeley- USF dataset. The FDT of the proposed DS detection method is 0.51ms as an average value on the set of USF images in Mendeley dataset.

Table 6. Fetus Detection Time (FDT) computations using the proposed DDS framework model- Mendeley- USF dataset

Methodologies	FDT in ms
Proposed DDS framework	**0.51**
Deep Learning-based Architecture	0.87
Non-invasive DS Detection	0.98
Swin Transformer for DS Detection	1.1
Modified Machine Learning Method	1.6
Deep Learning Measurement Model	1.9

Table 7 is the FDT computations using the proposed DDS framework model- KF- USF dataset. The FDT of the proposed DS detection method is 0.46ms as an average value on the set of USF images in Mendeley dataset.

Table 7. FDT computations using the proposed DDS framework model- KF- USF dataset

Methodologies	FDT in ms
Proposed DDS framework	**0.46**
Deep Learning-based Architecture	0.78
Non-invasive DS Detection	0.89
Swin Transformer for DS Detection	0.99
Modified Machine Learning Method	1.6
Deep Learning Measurement Model	1.98

The dataset splitting ratio for the NT region of abnormal USF images, with respect to incorrect classifications, indicates that the Mendeley and KF datasets exhibit only about 0.74% and 0.725% misclassified samples respectively, reflecting over 99% correct detection performance across both datasets.

CONCLUSION

This study suggests a complete automated process of Down Syndrome (DS) detection based on the ultrasound fetus (USF) images to overcome the weaknesses of the conventional invasive diagnostic procedures. The presented methodology is based on Non-Sub Sampled Contourlet Transform (NSCT) as the feature extraction utility and the Convolutional Neural Network (CNET) as the classifier, demonstrating good performance and efficiency. The system was very accurate in classifying two sets of data. The system had a high sensitivity, specificity, and accuracy on the Mendeley dataset in identifying abnormal USF images. The Fetal NT Sensitivity (FNSE) was 99.24, Fetal NT Specificity (FNSP) was 99.19 and the total Fetal NT Accuracy (FNA) was 99.23. On the same note, the KF data set recorded excellent outcomes, having FNSE of 99.24% and FNSP of 99.33, which highlighted the strength of the system with various sources of data. Moreover, the mean Fetus Detection Time (FDT) was 0.51 ms in the case of Mendeley and 0.46 ms in the case of KF dataset, which proves the efficiency of the system to be used in real-time. These findings underscore the potential of the proposed system as an effective, non-invasive screening system in the early detection of DS so that individuals do not face the risks of having to resort to the conventional diagnostic techniques which have adverse effects like miscarriage. The sensitivity, accuracy and speed of the system render the system very appropriate in clinical use. Future studies may address improving the strength of the system by adding additional imaging modalities, including MRI, and improving the model to process lower-resolution and noisy images. Generalizing the model and making it available to a wider variety of conditions of the fetus would make the models better.

REFERENCES

[1]   van der Meij KR, Henneman L, Sistermans EA. Non-invasive prenatal testing for everybody or contingent screening. Prenatal Diagnosis. 2023 Apr 1;43(4):443-7. https://doi.org/10.1002/pd.6296
[2]   Xie HN, Wang N, He M, Zhang LH, Cai HM, Xian JB, Lin MF, Zheng J, Yang YZ. Using deep-learning algorithms to classify fetal brain ultrasound images as normal or abnormal. Ultrasound in Obstetrics & Gynecology. 2020 Oct;56(4):579-87. https://doi.org/10.1002/uog.21967
[3]   Kumar S, Selvakumar K. Various Methods for Computing Risk Factors of Down Syndrome in Fetus. Archives of Computational Methods in Engineering. 2025 Jan;32(1):485-98.
[4]   Ye C, Duan H, Liu M, Liu J, Xiang J, Yin Y, Zhou Q, Yang D, Yan R, Li R. The value of combined detailed first-trimester ultrasound–biochemical analysis for screening fetal aneuploidy in the era of non-invasive prenatal testing. Archives of Gynecology and Obstetrics. 2024 Aug;310(2):843-53.
[5]   Micucci M, Iula A. Recent advances in machine learning applied to ultrasound imaging. Electronics. 2022 Jun 6;11(11):1800. https://doi.org/10.3390/electronics11111800
[6]   Thomas MC, Arjunan SP. Deep learning measurement model to segment the nuchal translucency region for the early identification of down syndrome. Measurement Science Review. 2022 May 14;22(4):187-92. https://doi.org/10.2478/msr-2022-0023
[7]   Bowden B, de Souza S, Puchades A, Williams K, Morgan S, Anderson S, Tucker D, Hillier S. Implementation of non-invasive prenatal testing within a national UK antenatal screening programme: Impact on women's choices. Prenatal Diagnosis. 2022 May;42(5):549-56. https://doi.org/10.1002/pd.6131
[8]   Yousefpour Shahrivar R, Karami F, Karami E. Enhancing fetal anomaly detection in ultrasonography images: a review of machine learning-based approaches. Biomimetics. 2023 Nov 2;8(7):519. https://doi.org/10.3390/biomimetics8070519
[9]   Zhang M, Gao Y, Liang M, Wang Y, Guo L, Wu D, Xiao H, Lin L, Wang H, Liao S. Correlation between maternal serum biomarkers and the risk of fetal chromosome copy number variants: a single-center retrospective study. Archives of Gynecology and Obstetrics. 2024 Aug;310(2):933-42.
[10]   Stallings EB, Isenburg JL, Rutkowski RE, Kirby RS, Nembhard WN, Sandidge T, Villavicencio S, Nguyen HH, McMahon DM, Nestoridi E, Pabst LJ. National population-based estimates for major birth defects, 2016–2020. Birth defects research. 2024 Jan;116(1):e2301. https://doi.org/10.1002/bdr2.2301
[11]   Raza A, Munir K, Almutairi MS, Sehar R. Novel transfer learning based deep features for diagnosis of down syndrome in children using facial images. IEEE Access. 2024 Jan 29;12:16386-96. https://doi.org/10.1109/ACCESS.2024.3359235
[12]   Tang J, Han J, Xue J, Zhen L, Yang X, Pan M, Hu L, Li R, Jiang Y, Zhang Y, Jing X. A deep-learning-based method can detect both common and rare genetic disorders in fetal ultrasound. Biomedicines. 2023 Jun 19;11(6):1756. https://doi.org/10.3390/biomedicines11061756
[13]   Geppert J, Stinton C, Johnson S, Clarke A, Grammatopoulos D, Taylor-Phillips S. Antenatal screening for fetal trisomies using microarray-based cell-free DNA testing: a systematic review and meta-analysis. Prenatal Diagnosis. 2020 Mar;40(4):454-62. https://doi.org/10.1002/pd.5621

[14] Devisri B, Kavitha M. Fetal growth analysis from ultrasound videos based on different biometrics using optimal segmentation and hybrid classifier. Statistics in Medicine. 2024 Feb 28;43(5):1019-47. https://doi.org/10.1002/sim.9995

[15] Khan IU, Aslam N, Anis FM, Mirza S, AlOwayed A, Aljuaid RM, Bakr RM, Qahtani NH. Deep learning-based computer-aided classification of amniotic fluid using ultrasound images from Saudi Arabia. Big Data and Cognitive Computing. 2022 Oct 3;6(4):107. https://doi.org/10.3390/bdcc6040107

[16] Abdullah D. Uncertainty-Aware Representation Learning with Physical Consistency for Robust Decision Processes in Large-Scale Data Systems. Journal of Scalable Data Engineering and Intelligent Computing. 2025 Sep 24:9-17. https://doi.org/10.17051/JSDEIC/02.03.02

[17] Koul AM, Ahmad F, Bhat A, Aein QU, Ahmad A, Reshi AA, Kaul RU. Unraveling Down syndrome: from genetic anomaly to artificial intelligence-enhanced diagnosis. Biomedicines. 2023 Dec 12;11(12):3284. https://doi.org/10.3390/biomedicines11123284

[18] Reshi AA, Shafi S, Qayoom I, Wani M, Parveen S, Ahmad A. Deep learning-based architecture for down syndrome assessment during early pregnancy using fetal ultrasound images. International Journal of Experimental Research and Review. 2024;38:182-93. https://doi.org/10.52756/ijerr.2024.v38.017

[19] Alzubaidi M, Agus M, Alyafei K, Althelaya KA, Shah U, Abd-Alrazaq A, Anbar M, Makhlouf M, Househ M. Toward deep observation: A systematic survey on artificial intelligence techniques to monitor fetus via ultrasound images. Iscience. 2022 Aug 19;25(8). https://doi.org/10.1016/j.isci.2022.104713

[20] Selvathi D, Chandralekha R. Fetal biometric based abnormality detection during prenatal development using deep learning techniques. Multidimensional systems and signal processing. 2022 Mar;33(1):1-5.

[21] Wang C, Yu L, Su J, Mahy T, Selis V, Yang C, Ma F. Down syndrome detection with swin transformer architecture. Biomedical Signal Processing and Control. 2023 Sep 1;86:105199. https://doi.org/10.1016/j.bspc.2023.105199

[22] Liu L, Tang D, Li X, Ouyang Y. Automatic fetal ultrasound image segmentation of first trimester for measuring biometric parameters based on deep learning. Multimedia Tools and Applications. 2024 Mar;83(9):27283-304.

[23] Abdullah D. Recent advancements in nanoengineering for biomedical applications: A comprehensive review. Innovative Reviews in Engineering and Science. 2024;1(1):1-5.

[24] Mengistu AK, Assaye BT, Flatie AB, Mossie Z. Detecting microcephaly and macrocephaly from ultrasound images using artificial intelligence. BMC Medical Imaging. 2025 May 26;25(1):183.

[25] Saranya S, Sudha S. Certain Mathematical Investigations on Prenatal Down Syndrome Detection using ANFIS Classification Approach. Appl. Math. 2020;14(1):97-104.